Appl. Phys. B 56, 34–38 (1993)

Applied Physics B Photophysics and Laser Chemistry

Spatio-Temporal Analysis of All-Optical Streaking

S. G. Dinev, A. A. Dreischuh, and I. M. Ivanova

Department of Physics, Sofia University, BG-1126 Sofia, Bulgaria (Fax: +359-2/463589)

Received 24 February 1992/Accepted 28 September 1992

Abstract. All-optical streaking in a cubic nonlinear medium is analyzed theoretically. The model based on the variational method employs the induced phase front distortion on a probe beam. The numerical calculations for a planar inert-gas filled waveguide show that on-line measurements of picosecond pulse durations in the short-wavelength region are possible.

PACS: 42.65, 42.80, 42.60.E

The progress in laser technology, including laser design, nonlinear optical materials and fiber optics, enable the generation of ultrashort laser pulses from the infrared to the ultraviolet region [1, 2]. Recently, the possibility of using the induced phase modulation (IPM) [3] with a subsequent pulse compression [4, 5] was proposed as a possible mean for achieving ultrashort pulses in the VUV spectral range [6]. The IPM has been considered as a method for induced focusing [7], collimation [8], light bullet formation [9], and all-optical beam deflection [10, 11]. Progress has been achieved in the development of a variety of methods for pulse duration measurement [12]. A commonly used technique in the UV is the single-shot and multiple-shot autocorrelation method based on multiphoton ionization/fluorescence [13].

In this paper we analyze theoretically the spatio-temporal dynamics of the induced deflection of an off-axial probe beam [10]. On this base we propose a novel technique for measuring pulse widths. In view of the recent experimental results reported [11], this idea seems feasible. In a planar waveguide containing a proper inert gas as a nonlinear medium, such a device would combine the fast nonlinear response of the electronic nonlinearity with the possibility for measuring pulse widths in the short-wavelength region.

Theoretical Model

The nonlinear medium considered is taken to be homogeneous, stationary and with a resonant structure. The last assumption is made to retain the possibility for achieving the pure effect of pump-induced probe beam deflection, although it is not obligatory [10, 11]. The copropagating beams are coherent, although in a nonresonant medium this is not necessary [14]. Choosing the probe- and pump-wavelengths λ_s and λ_p in the vicinity of $\lambda_s + \lambda_p$ two-photon resonance, one can obtain high values of the nonlinear susceptibility for IPM ($\chi^{(3)}_{\mathrm{IPM}}$). When the diffraction is limited to one transversal dimension (as in a planar, gas-filled optical waveguide), the system of coupled ordinary differential equations describing the spatio-temporal evolution of the probe and pump beam/pulse have the form

$$\mathrm{i}\,\frac{\partial\psi_s}{\partial x} + \alpha_s\frac{\partial^2\psi_s}{\partial\tau^2} + \beta_s\frac{\partial^2\psi_s}{\partial r^2} + k^{\mathrm{IPM}}(\lambda_s)\,|\psi_p|^2\psi_s = 0\,, \tag{1a}$$

$$\mathrm{i}\,\frac{\partial\psi_p}{\partial x} + \alpha_p\frac{\partial^2\psi_p}{\partial\tau^2} + \beta_p\frac{\partial^2\psi_p}{\partial r^2} + k^{\mathrm{SPM}}(\lambda_p)\,|\psi_p|^2\psi_p = 0\,. \tag{1b}$$

In these equations ψ_s and ψ_p are the slowly-varying envelope amplitudes of the probe and pump beam/pulse, respectively, $\alpha_{s\,p} = (-1/2)[\lambda^3_{s,p}/2\pi c^2)]\,[\partial^2 n/\partial\lambda^2]_{\lambda=\lambda_{s,p}}$ is the group-velocity dispersion (GVD) coefficient, $\beta_{s,p} = 1/(2k_{s,p})$, $k_{s,p}$ is the corresponding wave-number,

$$k^{\mathrm{IPM}}(\lambda_s) = \frac{n_2^{\mathrm{IPM}}(\lambda_s)\,k_s}{2n_{os}} = \frac{k_s}{2n_{os}}\,\frac{6\pi N\chi^{(3)}_{\mathrm{IPM}}(\lambda_s)}{n_{os}} \tag{2a}$$

and

$$k^{\mathrm{SPM}}(\lambda_p) = \frac{n_2^{\mathrm{SPM}}(\lambda_p)\,k_p}{2n_{op}} = \frac{k_p}{2n_{op}}\,\frac{3\pi N\chi^{(3)}_{\mathrm{SPM}}(\lambda_p)}{n_{op}} \tag{2b}$$

are the nonlinear coefficients for IPM of the probe pulse and self-phase modulation (SPM) for the pump pulse, N is the particle density, $\chi^{(3)}$ is the corresponding nonlinear susceptibility, $n_{os,p}$ are the refractive indexes, and r denotes the transverse diffraction non-limited coordinate.

The trial functions are chosen to be Gaussian in both time and space

$$\psi_S(x,r,\tau) = \frac{A_s(x)}{\omega_s(x)} \exp\left[-\frac{(\tau-\tau_D-x\nu_{SP})^2}{2\tau_s^2(x)} + ib_s(x)\tau^2\right] \times \exp\left[-\frac{[r-r_0(x)]^2}{a_s^2\omega_s^2(x)} - i\frac{k_s\varrho_s(x)r^2}{2}\right], \tag{3a}$$

$$\psi_P(x,r,\tau) = \frac{A_P(x)}{\omega_P(x)} \exp\left[-\frac{\tau^2}{2\tau_P^2(x)} + ib_P(x)\tau^2\right] \times \exp\left[-\frac{r^2}{a_P^2\omega_P^2(x)} - i\frac{k_P\varrho_P(x)r^2}{2}\right], \tag{3b}$$

and the spatio-temporal coordinate system is taken to be connected with the pump. In (3) A_S and A_P are the electric field amplitudes, ω_s and ω_p are the normalized beam radii, a_s and a_p are the physical beam radii at the entrance of the nonlinear medium, r_0 is the distance between the beam centers, ϱ_S and ϱ_P are the inverse of the radii of the probe/pump beam wavefront curvature, τ_s and τ_P are the half-pulse widths at $1/e$ level, b_P and b_S are the (self)induced chirp-rates for the pump/probe, τ_D is the eventual initial delay between the pulses, and $\nu_{SP} = (v_{GS}^{-1} - v_{GP}^{-1})$ accounts for the group-velocity mismatch.

If λ_s and λ_p are far from single- and two-photon resonances, the SPM is negligible compared to the IPM $[\chi^{(3)}_{SPM}(\lambda_{s,p}) \ll \chi^{(3)}_{IPM}]$. Therefore, the nonlinear term in (1b) can be neglected. If we assume a negligible self-action of the pump, the evolution of the pump beam radius and the pump pulse duration are given by the well-known relations [1]

$$\omega_p(x) = [1 + (x/L_{Dp})^2]^{1/2}, \tag{4a}$$

$$\tau_p(x) = \tau_p(x=0)[1 + (x/L'_{Dp})^2]^{1/2}, \tag{4b}$$

where $L_{Dp} = k_p a_p^2(x=0)/2$ is the Rayleigh diffraction length and $L'_{Dp} = \tau_p^2(x=0)/(2|\alpha_p|)$ is the dispersion length.

Let us now analyse the behavior of the probe beam. The initial conditions for the parameters of interest are $\omega_s(x=0) = 1$ and $\varrho_s(x=0) = 0$. The mathematical description of the probe beam evolution is based on the variational approach for solving (1a) [15]. The analytical form of the results is the main advantage of this method, which results in a set of ordinary differential equations for the corresponding variational parameters

$$\frac{d\omega_s}{dx} = -\omega_s\varrho_s, \tag{5a}$$

$$\frac{dr_0}{dx} = 2r_0\varrho_s, \tag{5b}$$

$$\frac{d\varrho_s}{dx} = \varrho_s^2 - \frac{4}{k_s^2a_s^4\omega_s^4} + \frac{4k^{IPM}(\lambda_s)|A_p|^2a_p}{\omega_pk_s(a_s^2\omega_s^2+a_p^2\omega_p^2)^{3/2}} \times\left(1-\frac{4r_0^2}{a_s^2\omega_s^2+a_p^2\omega_p^2}\right)\exp\left(-\frac{2r_0^2}{a_s^2\omega_s^2+a_p^2\omega_p^2}\right) \times\frac{\tau_p}{(\tau_s^2+\tau_p^2)^{1/2}}\exp\left[-\frac{(\tau_D-x\nu_{SP})^2}{\tau_s^2+\tau_p^2}\right], \tag{5c}$$

$$\frac{d\tau_s}{dx} = 4\alpha_sb_s\tau_s, \tag{5d}$$

$$\frac{db_s}{dx} = -4\alpha_sb_s^2 + \frac{\alpha_s}{\tau_s^4} - \frac{k^{IPM}(\lambda_s)|A_p|^2a_p}{2\omega_p(a_s^2\omega_s^2+a_p^2\omega_p^2)^{1/2}}\frac{\tau_p}{(\tau_s^2+\tau_p^2)^{3/2}} \times\left[1-\frac{2(\tau_D-x\nu_{SP})^2}{\tau_s^2+\tau_p^2}\right]\exp\left[-\frac{(\tau_D-x\nu_{SP})^2}{\tau_s^2+\tau_p^2}\right] \times\exp\left(-\frac{2r_0^2}{a_s^2\omega_s^2+a_p^2\omega_p^2}\right). \tag{5e}$$

It is natural to expect that the spatio-temporal evolution of the probe beam/pulse depends crucially on the beam shapes. In Appendix A the corresponding variational results for sech-type trial functions are presented.

The physical mechanism of the induced deflection is the probe beam phase profile distortions induced by the pump [10, 11, 14]. It can be shown, (5b,c), that for Gaussian beam/pulse shapes, the condition

$$\mathrm{sign}\left[k^{IPM}(\lambda_s)\left(1-\frac{4r_0^2}{a_s^2\omega_s^2+a_p^2\omega_p^2}\right)\right] > 0 \tag{6}$$

corresponds to induced focusing and the opposite one – to induced defocusing. Therefore, the conditions under which induced probe beam deflection can occur, depend simultaneously on the sign of the nonlinear susceptibility, the beam radii and their initial physical separation. This result is important for extending the number of nonlinear media [10] appropriate for observing the effect proposed.

Figure 1 shows the evolution of the distance between the beam centers r_0 along the nonlinear medium in the case of $\Delta n = (1/2)n_2|E_p|^2 = -5.7\times10^{-5}$ (1 atm Xe, $\lambda_s = 264.42$ nm, $\lambda_p = 248$ nm, $I_p = 5\times10^8$ W/cm², $\chi^{(3)}_{IPM}(\lambda_s) = -5.8\times10^{-32}$ esu and Gaussian beam/pulse shapes). The same conditions are kept in the rest of this work. The nonlinear susceptibility is calculated according to the single-sided Feynman diagrams [16] and the accuracy,

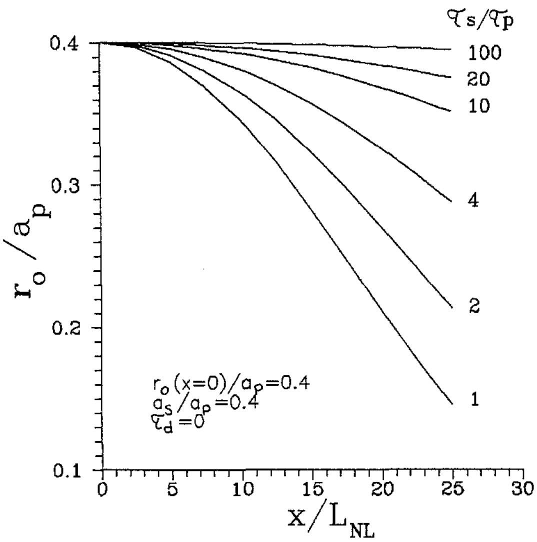

Fig. 1. Evolution of the distance between the beam centers r_0/a_p along the nonlinear medium. The parameters used are: nonlinear medium Xe (1 atm), $\lambda_s = 264.42$ nm, $\lambda_p = 248$ nm, $I_p = 5\times10^8$ W/cm², $\chi^{(3)}_{IPM}(\lambda_s) = -5.8\times10^{-32}$ esu, $\Delta n = -5.7\times10^{-5}$. The distance is normalized to the nonlinear length L_{NL}

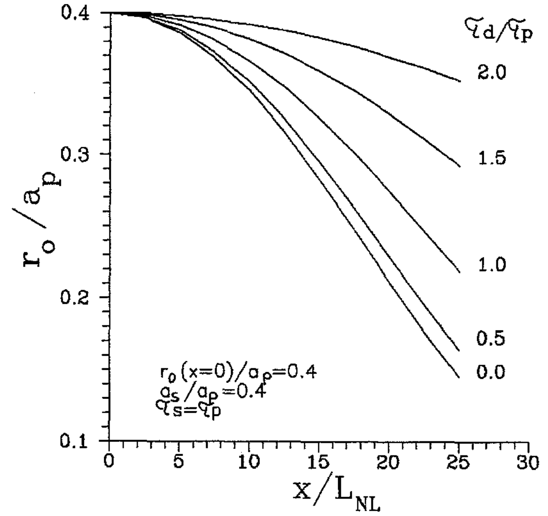

Fig. 2. Influence of the initial delay τ_D between the signal and the pump pulse on the distance between the beam centers r_0/a_p. The parameters are the same as in Fig. 1

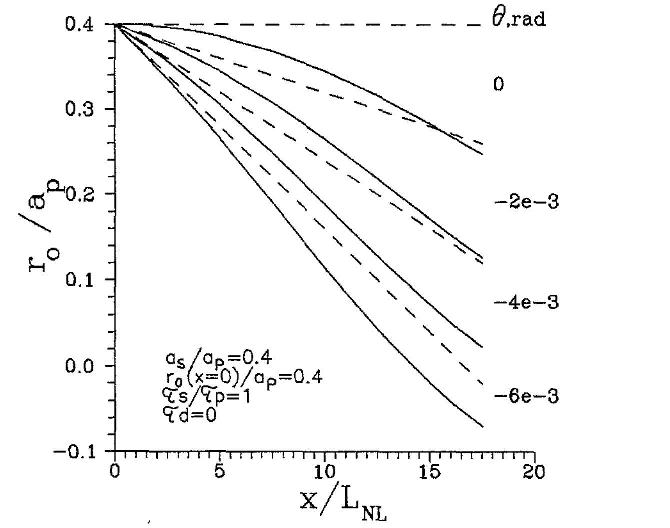

Fig. 3. Influence of the initial angular deviation θ between the signal and pump beams on the distance between the beam centers r_0/a_p (*solid line*). *Dashed line*: off-axis distance evolution in the absence of a pump. The parameters are the same as in Fig. 1

according to the accuracy of the dipole matrix elements used, was estimated to be 40%. For convenience, the longitudinal coordinate x is normalized to the nonlinear distance $L_{NL} = 1/|k^{IPM}(\lambda_s)|A_p|^2|$. As can be seen from the figure, with increasing the ratio of signal to pump pulse duration τ_s/τ_p the nonlinear propagation regime becomes weaker because of the decrease of the effective pulse overlap. Further, with increasing the initial time delay with respect to the pump pulse duration, the change rate of the distance between the beam centers r_0 decreases. This dependence is nonlinear with τ_d/τ_p (Fig. 2). The case $\tau_d \gg \tau_s, \tau_p$ corresponds to a linear propagation regime of two noninteracting beams, separated in time and space. In order to achieve a linear deflection of the probe beam, the length of the nonlinear medium x_{NL} should be restricted to the region of a nearly linear reduction of r_0 along the x-axis ($x_{NL} \approx 7$ cm, i.e. $x/L_{NL} \approx 17.5$ in the case considered; see Fig. 1). The spatial separation of the two beams outside the nonlinear medium can be performed by introducing a small initial angular deviation $\theta = (dr_0/dx)_{x=0}$. In this case (5b) should be transformed to

$$\frac{dr_0}{dx} = \theta + 2r_0\varrho_s\,. \tag{7}$$

Figure 3 plots the dependence $r_0(x)$ for different values of θ (solid lines). The dashed lines represent the evolution of the distance between the beam centers in the absence of a pump. As seen from the figure, with increasing the initial angle θ between the beams, the contrast between the corresponding pairs of curves decreases. Therefore, it should be kept reasonably small [11].

Since the method is fundamentally based on nonlinear spatial interaction of two beams, one would expect that the spatial distribution of the beams plays an important role, but the energy redistribution in the transverse cross-section of the probe beam could not be accounted for within the variational description presented. Figure 4 plots the evolution of the distance between the beam centers $r_0(x)/a_p$ along the nonlinear medium for Gaussian-(curves 1) and

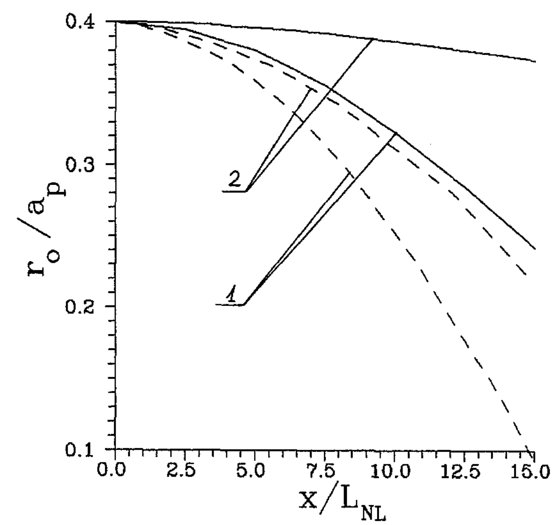

Fig. 4. Evolution of the distance between the beam centers r_0/a_p along the nonlinear medium for Gaussian- (*curves 1*) and sech-shaped beams (*curves 2*). *Solid lines*: variational results; *dashed lines*: numerical results. The parameters are the same as in Fig. 1

sech-shaped beams (curves 2). These curves are obtained by solving (1) numerically (dashed lines), using the split-step Fourier method. For comparison, the solid curves represent the variational results [see Fig. 2, the lowest curve, (5a–5e) and (A3–A6)]. As seen from Fig. 4, under the same initial conditions, the numerical results for sech-shaped beams are close to the variational predictions for Gaussian beams. Generally speaking, because of the energy redistribution and the shape-changes, the numerical results for Gaussian- and sech-shaped beams are much more optimistic and accurate. It should be noted, that the results for sech-trial functions in space are calculated under the optimum initial conditions for deflection of Gaussian beams. The optimum conditions for sech-beam profiles seem difficult to obtain in an analytical form (see Appendix A). Generally, at a certain delay only that part of the probe pulse overlapping with the pump pulse will be deflected. Exiting the nonlinear medium, the probe beam may develop oscillatory wings, as a result of the optical wave-breaking [11]. Under this probe beam/pulse distortion, the probe beam center should be attributed to the mostly deviated maximum in the temporally-averaged probe beam profile [11]. It should be noted that in the practical cases considered [10, 11] this peak strongly dominates the oscillatory wing of the deflected beam.

In view of the above mentioned results, we will try to propose an experimental arrangement for measuring pump pulse durations based on the induced probe beam deflection in an off-axis geometry. The potential experimental setup is shown in Fig. 5a. The two incoming beams, the pump (to be measured in time) and the probe beam, enter the nonlinear medium with a length x_{NL}, having an initial axis separation $r_0(x=0)$ and an initial angular deviation θ. A linear diode array placed in a proper distance L_{M} from the entrance of the medium, can be used for determining the position of the probe beam center in the plane of measurement. This distance should be large enough for an effective angular separation of the beams. Figure 5b shows the results for the normalized beam separation evolution $r_0(x)/a_{\mathrm{p}}$, obtained by solving (5a–c) under the simplifying assumption that the pulse durations and their mutual temporal disposition does not change significantly inside the nonlinear medium ($\tau_{\mathrm{d}} \approx 0$ and $\nu_{\mathrm{sp}} \approx 0$). For the numerical example we have chosen $x_{\mathrm{NL}} = 7\,\mathrm{cm}$, $(a_{\mathrm{s}}/a_{\mathrm{p}})|_{x=0} = 0.4$, $(r_0/a_{\mathrm{p}})|_{x=0} = 0.4$, $\theta = -2 \times 10^{-3}\,\mathrm{rad}$, $L_{\mathrm{M}} = 100\,\mathrm{cm}$, $\Delta n = (1/2)n_2|E_{\mathrm{p}}|^2 = -5.7 \times 10^{-5}$, $\tau_{\mathrm{s}} = \tau_{\mathrm{p}} = 10\,\mathrm{ps}$. The dashed line represents the linear propagation of the probe beam without influence from the pump. The solid curves correspond to the probe beam propagation for different values of the initial delay τ_{d} with respect to the pump pulse duration. As expected, the presence of a pump leads to a maximum probe beam deviation at $\tau_{\mathrm{d}} = 0$, whereas at $\tau_{\mathrm{d}} = 5\tau_{\mathrm{p}}$ the probe beam propagation is practically the same as in the linear case. It should be noticed, that the dependence of the probe beam center position at the linear diode array is not linear with respect to $\tau_{\mathrm{d}}/\tau_{\mathrm{p}}$. The resolution of this position will be limited by the spatial resolution of the position sensitive detector (typically 25 µm).

For practical use it is necessary to derive an approximate analytical relationship, appropriate for a fast deduction of the pump pulse duration. At $\tau_{\mathrm{d}} \gg \tau_{\mathrm{s}}, \tau_{\mathrm{p}}$, the probe beam phase front distortions are negligible and it continues to propagate as a plane wave ($\varrho_{\mathrm{s}}(x) = 0$, $dr_0/dx = \theta$). Therefore, (5c) can be rewritten in the form

$$D\,\frac{\omega_{\mathrm{p}}(a_{\mathrm{s}}^2\omega_{\mathrm{s}}^2 + a_{\mathrm{p}}^2\omega_{\mathrm{p}}^2)^{3/2}}{a_{\mathrm{s}}^4\omega_{\mathrm{s}}^4 k_{\mathrm{s}}|k^{\mathrm{IPM}}(\lambda_{\mathrm{s}})|\,|A_{\mathrm{p}}|^2 a_{\mathrm{p}}} = \beta\,\frac{\tau_{\mathrm{p}}}{(\tau_{\mathrm{s}}^2+\tau_{\mathrm{p}}^2)^{1/2}}\exp\left[-\frac{\tau_{\mathrm{d\,max}}^2}{(\tau_{\mathrm{s}}^2+\tau_{\mathrm{p}}^2)}\right], \tag{8a}$$

where

$$D = \left(1 - \frac{4r_0^2}{a_{\mathrm{s}}^2\omega_{\mathrm{s}}^2 + a_{\mathrm{p}}^2\omega_{\mathrm{p}}^2}\right)^{-1}\exp\left(\frac{2r_0^2}{a_{\mathrm{s}}^2\omega_{\mathrm{s}}^2 + a_{\mathrm{p}}^2\omega_{\mathrm{p}}^2}\right). \tag{8b}$$

In (8a) $\tau_{\mathrm{d\,max}}$ is the maximum initial temporal delay between the pulses, for which the linear and the nonlinear probe beam propagation regime cannot be resolved and β is a constant

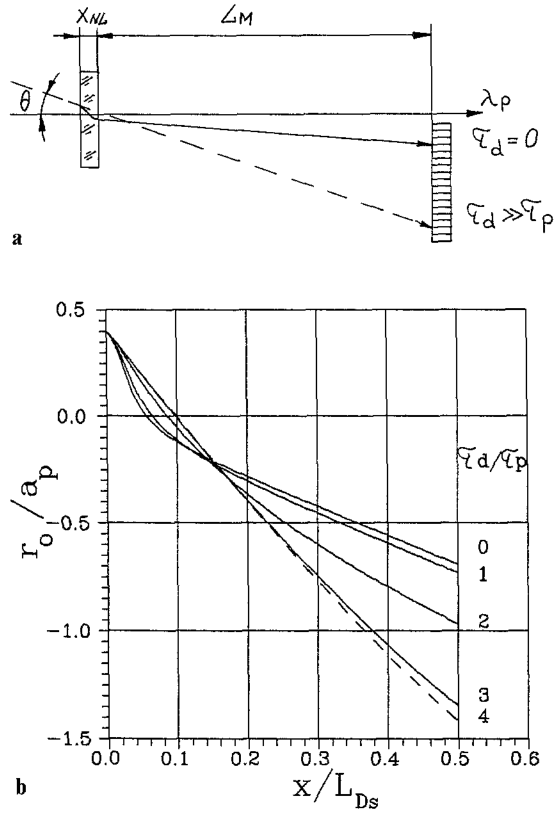

Fig. 5. a A proposed experimental setup for all-optical streaking using induced phase-front distortions; **b** Signal beam deviation r_0/a_{p} as a function of distance x/L_{DS} to the position-sensitive detector for different initial delays τ_{D}. $x_{\mathrm{NL}} = 7\,\mathrm{cm}$, $(a_{\mathrm{s}}/a_{\mathrm{p}})|_{x=0} = 0.4$, $(r_0/a_{\mathrm{p}})|_{x=0} = 0.4$, $\theta = -2 \times 10^{-3}\,\mathrm{rad}$, $L_{\mathrm{M}} = 100\,\mathrm{cm}$, $\Delta n = (1/2)n_2|E_{\mathrm{p}}|^2 = -5.7 \times 10^{-5}$, $\tau_{\mathrm{s}} = \tau_{\mathrm{p}} = 10\,\mathrm{ps}$ and $L_{\mathrm{DS}} = 200\,\mathrm{cm}$. *Dashed line*: linear propagation of the signal beam without a pump

($\beta \gg 1$ corresponds to a dominating diffraction divergence). Let us introduce the notation $\gamma = [a_{\mathrm{p}}\omega_{\mathrm{p}}/(a_{\mathrm{s}}\omega_{\mathrm{s}})]|_{x=0}$. Making use of the relations

$$|A_{\mathrm{p}}|^2 = 8\pi I_{\mathrm{p}}/(cn_{0\mathrm{s}}) \tag{9a}$$

and

$$P_{\mathrm{CRIT}}^{\mathrm{IF}} = \frac{(1+\gamma^2)^{3/2}}{2\sqrt{2}\gamma}\,\frac{\sqrt{2}c\lambda_{\mathrm{s}}^2 n_{0\mathrm{s}}^2}{8\pi^2|n_2^{\mathrm{IPM}}(\lambda_{\mathrm{s}})|}, \qquad N_{\mathrm{p}} = P_{\mathrm{p}}/P_{\mathrm{CRIT}}^{\mathrm{IF}}, \tag{9b}$$

one can derive an alternative form of (8), namely:

$$\frac{(1+\gamma^2)^{3/2}}{2\sqrt{2}\gamma}\,\frac{D}{N_{\mathrm{p}}} = \beta\,\frac{\tau_{\mathrm{p}}}{(\tau_{\mathrm{s}}^2+\tau_{\mathrm{p}}^2)^{1/2}}\exp\left[-\frac{\tau_{\mathrm{d\,max}}^2}{(\tau_{\mathrm{s}}^2+\tau_{\mathrm{p}}^2)}\right]. \tag{10}$$

In (9) $P_{\mathrm{CRIT}}^{\mathrm{IF}}$ is the critical power for induced focusing (IF) of a probe beam, on-axially aligned to the pump beam. The term comprising γ reflects the enhancement of the critical power for IF at $\gamma = [a_{\mathrm{p}}\omega_{\mathrm{p}}/(a_{\mathrm{s}}\omega_{\mathrm{s}})] > 1$ due to the reduced refractive index change over the cross-section of the probe beam [17]. The quantity $\beta N_{\mathrm{p}}/D$ can be obtained by a calibrating measurement of $\tau_{\mathrm{d\,max}}$ (Fig. 5b) with pump and probe pulses of same duration. Using a reference channel for the pump to eliminate the pulse-to-pulse instabilities from the experimental conditions one can deduce the value of β for the particular position-sensitive detector. The numerical calculation, according to (10), at $\tau_s = \tau_p = 10\,\mathrm{ps}$, $(a_s/a_p)|_{x=0} = 0.4$, $(r_0/a_p)|_{x=0} = 0.4$, $\theta = -2 \times 10^{-3}\,\mathrm{rad}$, $\gamma = 2.5$, and $N_p = 2$ (see Fig. 4, solid curve 1) gives a value of $(\beta/D) = 516$. If $\tau_s/\tau_p = 10$, the relative error between the results of (10) and (5) is within 10%. In our opinion, this is the typical inaccuracy of the analytical approximate relation, given by (9), compared to the variational results (5).

As can be seen from Fig. 5b, by the set of parameters considered and 1 mrad probe-beam deflection, the variational approach predicts an accuracy of the order of 30%. In contrast, the numerical method which can account for the beam profile evolution by the same set of parameters predicts a measurement accuracy of better than 5%. Unfortunately, the estimation of the temporal form of the measured pulse, possible in an streak-camera measurement, seems impossible.

Conclusion

In a medium with cubic nonlinearity the pump-induced probe beam phase front distortions can be used to achieve all-optical streaking. A variational model of the spatio-temporal dynamics of this process is presented, resulting in a set of differential equations for Gaussian- and sech-beam profiles. A novel technique for measuring pulse widths based on the induced deflection of an off-axis probe beam copropagating with the pump beam is proposed. A simple analytical expression is derived for an on-line deduction of the pump pulse duration at the expense of an inaccuracy within 10%. With a proper inert gas as a nonlinear medium, such a device would combine the fast response of the electronic nonlinearity with the possibility for measuring pulse widths in the short-wavelength region. The method discussed can also find application in all-optical deflectors, modulators, memory and switching devices. The progress in tunable ultrashort sources, especially those based on solid state/semiconductor materials seems to make the idea of all-optical deflection in the short-wavelength region viable. A device based on this principle seems to be realizable and relatively simple.

Appendix A

According to the notations introduced, the pump and probe beams are assumed to be of sech-type:

$$\psi_S(x,r,\tau) = \frac{A_s(x)}{\omega_S(x)} \exp\left[-\frac{(\tau-\tau_D-x\nu_{SP})^2}{2\tau_s^2(x)} + ib_s(x)\tau^2\right] \times \operatorname{sech}\left[\frac{r-r_0(x)}{a_S\omega_S(x)}\right] \exp\left[-i\,\frac{k_S\varrho_S(x)r^2}{2}\right], \tag{A1}$$

$$\psi_P(x,r,\tau) = \frac{A_P(x)}{\omega_P(x)} \exp\left[-\frac{\tau^2}{2\tau_P^2(x)} + ib_P(x)\tau^2\right] \times \operatorname{sech}\left[\frac{r}{a_P\omega_P(x)}\right] \exp\left[-i\,\frac{k_P\varrho_P(x)r^2}{2}\right], \tag{A2}$$

Applying the variational procedure, we obtain a system of differential equations. Three of them, $d\omega_S/dx$, dr_0/dx, and $d\tau_S/dx$, are identical to (5a), (5b), and (5d), respectively, and

$$\frac{d\varrho_s}{dx} = \varrho_s^2 - \frac{4}{\pi^2 k_s^2 a_s^4 \omega_s^4} - \frac{6k^{\mathrm{IPM}}(\lambda_s)\,|A_p|^2}{\pi^2 k_s a_s^3 \omega_s^3 \omega_p^2}(B-G) \times \frac{\tau_p}{(\tau_s^2+\tau_p^2)^{1/2}} \exp\left[-\frac{(\tau_D - x\nu_{SP})^2}{\tau_s^2+\tau_p^2}\right], \tag{A3}$$

$$\frac{db_s}{dx} = -4\alpha_s b_s^2 + \frac{\alpha_s}{\tau_s^4} - \frac{k^{\mathrm{IPM}}(\lambda_s)\,|A_p|^2 B}{2a_s\omega_s\omega_p^2}\,\frac{\tau_p}{(\tau_s^2+\tau_p^2)^{3/2}} \times \left[1 - \frac{(\tau_D - x\nu_{SP})^2}{\tau_s^2+\tau_p^2}\right] \exp\left[-\frac{(\tau_D - x\nu_{SP})^2}{\tau_s^2+\tau_p^2}\right], \tag{A4}$$

where

$$B = \int_{-\infty}^{+\infty} \operatorname{sech}^2\left[\frac{r}{a_P\omega_P(x)}\right] \operatorname{sech}^2\left[\frac{r-r_0(x)}{a_S\omega_S(x)}\right] dr\,, \tag{A5}$$

$$G = \int_{-\infty}^{+\infty} \operatorname{sech}^2\left[\frac{r}{a_P\omega_P(x)}\right] \operatorname{sech}^2\left[\frac{r-r_0(x)}{a_S\omega_S(x)}\right] \times \operatorname{sh}\left[\frac{r-r_0(x)}{a_S\omega_S(x)}\right]\left[\frac{r-r_0(x)}{a_S\omega_S(x)}\right] dr\,. \tag{A6}$$

Unfortunately, the integrals have an analytical solution at small distances between the beam centers only $[r_0(x) \ll a_S\omega_S(x),\ a_P\omega_P(x)]$.

Acknowledgements. The authors would like to acknowledge the financial support of this research by National Foundation "Young Scientist", Bulgaria under contract # MU-TT-1/1991.

References

1. For a review see: G.P. Agarwal: *Nonlinear Fiber Optics* (Academic, Boston 1989)
2. J.D. Simon: Rev. Sci. Instrum. **60**, 3597–3624 (1989) and references therein
3. J.T. Manassah, M.A. Mustafa, R.R. Alfano, P.P. Ho: Phys. Lett. A **113**, 242–247 (1985)
   R.R. Alfano, Q. Li, T. Jimbo, J. Manassah, P.P. Ho: Opt. Lett. **11**, 626–628 (1986)
4. J.T. Manassah: Opt. Lett. **13**, 755–757 (1988)
5. B.H. Kolner: In *Ultrafast Phenomena VI,* ed. by T. Yajima, K. Yoshihara, C.B. Harris, S. Shionoya, Springer Ser. Chem. Phys. Vol. 48 (Springer, Berlin, Heidelberg 1988) pp. 47–49
6. S.G. Dinev, A.A. Dreischuh: J. Phys. B **24**, 319–323 (1991)
7. J.T. Manassah: Opt. Lett. **14**, 396–398 (1988)
8. S.G. Dinev, A.A. Dreischuh, D. Kavaldjiev, K. Krastev: J. Opt. Soc. Am. B **9**, 387–390 (1992)
9. A.B. Blagoeva, S.G. Dinev, A.A. Dreischuh, A.M. Naidenov: IEEE J. QE-**27**, 2060–2065 (1991)
10. G.P. Agrawal: Phys. Rev. Lett. **64**, 2487–2490 (1990)
11. A.J. Stenz, M. Kauranen, J.J. Maki, G.P. Agrawal, R.W. Boyd: Opt. Lett. **17**, 19–21 (1992)
12. For a review see S.L. Shapiro: In *Ultrafast Light pulses. Picosecond Techniques and Applications.* Topics Appl. Phys., Vol. 18 (Springer, Berlin, Heidelberg 1977)
13. A. Tünnermann, E. Eichmann, R. Henking, K. Mossavi, B. Wellegehausen: Opt. Lett. **16**, 402–403 (1991)
14. Y. Li, D.Y. Chen, L. Yang, R.R. Alfano: Opt. Lett. **16**, 438–440 (1990)
15. D. Anderson: Phys. Rev. A **27**, 3135–3145 (1983)
16. Y. Prior: IEEE J. QE-**20**, 27–42 (1984)
17. S.G. Dinev, A.A. Dreischuh, A.M. Naidenov: J. Opt. Soc. Am. B **8**, 2128–2132 (1991)